Molecular nature of resonant x-ray scattering in solid $LiNO_3$

A. B. Preobrajenski,[1,2,*] A. S. Vinogradov,[2] S. A. Krasnikov,[2,3] R. Szargan,[3] and N. Mårtensson[1]
[1]*MAX-lab, 22100 Lund, Sweden*
[2]*V.A. Fock Institute of Physics, St. Petersburg State University, 198504 St. Petersburg, Russia*
[3]*W.-Ostwald-Institut für Physikalische und Theoretische Chemie, Universität Leipzig, 04103 Leipzig, Germany*
(Received 10 November 2003; published 22 March 2004)

Resonant x-ray emission spectroscopy has been applied to study radiative decay processes following the N $1s$ near-edge excitations in solid $LiNO_3$. It has been shown that the origin of both nonresonant and resonant spectra are essentially molecular, their shape being primarily determined by the electron transitions between molecular orbitals of the quasiisolated NO_3^- anion. A strong low-energy sideband observed in the recombination spectrum following the N $1s^{-1}\pi^*$ excitation is attributed to the effect of dynamical x-ray emission accompanying the $D_{3h}\rightarrow C_{3v}$ distortion of the core-excited NO_3^- species.

DOI: 10.1103/PhysRevB.69.115116 PACS number(s): 71.20.−b, 78.70.Ck, 78.70.Dm, 78.70.En

I. INTRODUCTION

Electronic structure and resonant x-ray scattering (RXS) in solids are commonly described in terms of either localized or delocalized states depending on the system under study. Solids with valence bands composed of *s* and *p* electrons are usually considered as systems with weakly localized valence electrons and their RXS spectra are treated in the framework of energy-band models.[1,2] Due to weak localization of the valence electrons, band dispersion is usually strong in these systems making it possible to map valence-band structure by resonant inelastic x-ray scattering (RIXS) assuming that the crystal momentum does not change in the scattering process. In this manner RIXS was successfully used to describe details of the electronic structure in diamond,[1,3] graphite,[4,5] hexagonal BN (Refs. 5,6) and other *s*-*p* bonded materials, although the influence of core-hole effects on the quality of band mapping has been much discussed.[2,5,7,8] At the other extreme, systems with strong electron correlation (e.g., *d* and *f* metal compounds) can be characterized by strong localization of (a part of) electrons in the upper occupied states resulting in the narrow bands (e.g., bands composed of *d* and *f* states). Narrow bands imply weak dispersion, hence restricting crystal-momentum selectivity in RIXS. For such systems it is more appropriate to describe RIXS in terms of local approaches like atomic models or the Anderson impurity model, which consider the spectra as a result of interplay between intra-atomic multiplet coupling and interatomic hybridization.[9,10] Localized description of electronic structure and RXS was successful in such *d* and *f* electron systems as MnO,[11] CeO_2, UO_3,[12] Nd_2O_3,[13] and many others.

On the other hand, as soon as the solid under study contains quasi-isolated (quasimolecular) chemically stable atomic groups as its structural units, one can try to describe its electronic structure and processes of resonant excitation and deexcitation in terms of molecular orbitals of these groups. Recently we demonstrated that such quasimolecular approach can be highly instructive and helpful for understanding the processes of resonant nonradiative (Auger) decay in ionic-molecular crystals $M NO_2$ and $M NO_3$ (M = Li, Na).[14–16] In these solids the bonding between alkali-metal atom and NO_2 (NO_3) group is rather ionic, while inside the NO_2^- (NO_3^-) anion it is essentially covalent. Both spectator and participator decay channels were found to be quite intense as a consequence of strong localization of the π^* excitations on the NO_2 (NO_3) fragments. Furthermore, signatures of nuclear motion have been detected in the Auger decay spectra of the core-excited NO_3^- anion.[15,16] All these effects result from the essentially molecular nature of the highest occupied and lowest unoccupied electronic states in the ionic-molecular crystals.

Though sensitive enough for detecting molecular effects in the decay dynamics, resonant Auger (RA) spectra were too complicated for the unambiguous assignment of all spectral features in case of MNO_3.[15,16] On the other hand, resonant x-ray emission spectroscopy (RXES) can provide information, which is complementary to resonant Auger. An especially attractive feature of RXE spectroscopy in comparison with RA technique is a simpler spectral shape resulting from more strict selection rules. In this paper we apply RXES to the investigation of radiative decay processes following the N 1s near-edge excitations in the NO_3^- anion of solid $LiNO_3$. Our main goal is to understand whether the origin of main RIXS structures in the spectra of this ionic-molecular crystal can be explained in the framework of a quasimolecular approach in terms of electron transitions between molecular orbitals of the NO_3^- anion. From the analysis of evolution of the x-ray emission spectra upon tuning photon energy across the N 1s absorption edge we also extract information on the vibrational motion inside the core-excited NO_3^- group. In particular, we will demonstrate that an intense and structured tail observed at the low-energy side of the reemission peak upon sweeping photon energy across the N $1s\rightarrow 2a_2''$ resonance is a direct evidence of the dynamical x-ray emission inside core-excited NO_3^-.

II. EXPERIMENT

RXES measurements were performed at the ''bulk'' branch of the beamline I511 at MAX II storage ring in Lund, Sweden. The modified SX 700 monochromator of this beamline was operated with the photon-energy resolution of 0.17 eV at the *N* $1s$ edge and 0.25 eV at the O $1s$ edge. The soft

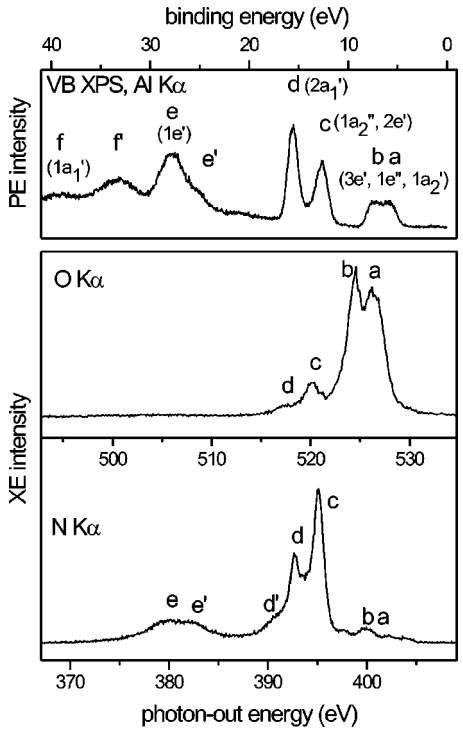

FIG. 1. Valence-band photoemission and nonresonant x-ray emission in $LiNO_3$. See text for energy alignment details.

x-ray absorption spectra were measured in the total electron yield mode and normalized to the incident photon flux. The x-ray emission spectra were recorded using a grazing-incidence x-ray spectrometer (XES 300 from Gammadata-Scienta) with the resolution of 0.45 eV at the N 1*s* edge and 0.6 eV at the O 1*s* edge. The optical axis of the x-ray spectrometer was set perpendicular to the beamline axis in the plane of polarization of the incident radiation in order to avoid Thompson scattering (in this geometry polarization vectors of incident and emitted radiation are perpendicular). The angle between the sample normal and the spectrometer axis was about 30. The powder samples (Alfa Aesar) were pressed into metallic indium attached to the sample holder. Since radiation damage was found to be noticeable after several hours of measurements, the area irradiated by the beam was changed every hour. The valence-band photoemission (PE) spectrum of $LiNO_3$ reported in this paper as well as the N 1*s* and O 1*s* photoelectron lines used for the energy alignment of the N 1*s* and O 1*s* nonresonant x-ray emission spectra were measured from an *in situ* evaporated thin $LiNO_3$ film with monochromatized Al Kα radiation using a VG Escalab 220iXL spectrometer at the Wilhelm-Ostwald-Institute for Physical and Theoretical Chemistry in Leipzig.

III. RESULTS AND DISCUSSION

The valence-band (VB) PE spectrum and the nonresonant (normal) N 1*s* and O 1*s* XES spectra of $LiNO_3$ are compared in Fig. 1. The binding energy (E_B) is measured relative to the Fermi level, and the alignment is performed using the measured values $E_B(N1s) = 408.06$ eV and $E_B(O1s) = 533.76$ eV. It should be noted that a comparison of the valence-band PE spectra with the normal (also x-ray excited) XES spectra for $LiNO_3$ was performed previously by Kosuch *et al.*[17] with a lower spectral resolution. However, our XES spectra are very different from those presented in Ref. 17, probably due to weaker radiation damage in our study. Indeed, the N 1*s* and O 1*s* x-ray emission spectra changed, over a period of several hours of irradiation, from looking similar to the spectra of Fig. 1 to looking similar to those published earlier.[17]

According to the dipole selection rule, the O 1*s* emission is roughly proportional to the O 2*p* density of states (DOS) and the N 1*s* emission to the N 2*p* DOS. It is evident from Fig. 1 that the uppermost VB structures, *a*-*b*, are composed of O 2*p* states with just a tiny admixture of N 2*p* states while the sharp peak *c* is mainly due to the N 2*p* DOS with some O 2*p* contribution. The O 2*s* and N 2*s* states yield the dominating contribution to peak *d*,[15,17] however some N 2*p* and O 2*p* admixtures give rise to the corresponding features in the N 1*s* and O 1*s* XE spectra. In the N 1*s* spectrum the surprisingly high intensity of peak *d* and appearance of shoulder d' may result from a contribution of the final-state shake-up satellites of peak *c*. As can be seen from Fig. 1, feature *e* also contains a rather strong contribution from the N 2*p* states. Structures e' and f' are probably due to the shake-up satellites, by analogy with the many-particle excitations observed in valence ionization of simple molecules.[18–20] Because of the essentially molecular character of the valence band (i.e., sharp and well separated structures) it is possible to assign all VB features to the molecular orbitals (MOs) of the NO_3^- anion (D_{3h} symmetry), as was done for $NaNO_3$.[15] In agreement with the MO calculations for NO_3^- (Refs. 21–23) the following assignment can be proposed (in order of increasing E_B): nonbonding $1a_2'$, nonbonding $1e''$, and weakly bonding $3e'$ MO's constitute band *a*-*b*, bonding $2e'$ and $1a_2''$ MO's give rise to peak *c*, bonding $2a_1'$ MO to peak *d*, and strongly bonding orbitals $1e'$ and $1a_1'$ are responsible for features *e* and *f*, respectively (Fig. 1). On the whole, six spectral features (*a*-*f*) are due to eight primary ionization processes and two spectral features (e' and f') are due to many-particle processes.

The N 1*s* x-ray absorption (XA) and emission spectra for $LiNO_3$ are shown in Fig. 2. The XA spectrum is rather similar to the B 1*s* spectrum for the gas-phase BF_3 molecule,[24] which is an isoelectronic and isostructural analogue of the NO_3^- anion. This fact confirms that the nature of the N 1*s* absorption in $LiNO_3$ is essentially molecular: it is determined mainly by the (highly anisotropic) potential of the NO_3 group. By analogy with the B 1*s* spectrum of BF_3 we assign the strong and slightly asymmetric band A below the ionization threshold to the N $1s^{-1}2a_2''(\pi^*)$ excitation and a broader band B-C above threshold to the N $1s^{-1}4e'(\sigma^*)$ excitation (in the D_{3h} point group notation). The structure of the latter band is caused probably by many-particle effects. The origin of shoulder B' is not quite clear. One can argue that a spontaneous symmetry breaking occurs in the core-excited NO_3^- anion reducing the symmetry from D_{3h} to C_{3v}, so that the N $1s \rightarrow 3a_1'$ transition (dipole forbidden in D_{3h}) borrows intensity from the N $1s \rightarrow 2a_2''$ transition via the a_2''

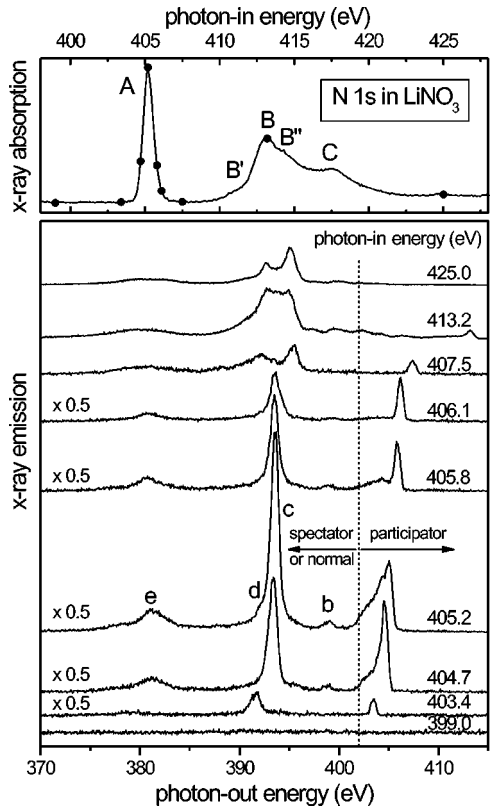

FIG. 2. N 1*s* absorption spectrum in $LiNO_3$ (upper panel); black dots indicate photon energies chosen for the excitation of resonant and nonresonant x-ray emission spectra (lower panel). Emission spectra are normalized to the acquisition time and the incoming photon flux. Vertical dashed line at $h\nu_{out}=402$ eV separates spectral features resulting from the spectator and/or normal radiative decay and participator decay.

(ν_2) out-of-plane vibration and manifests itself as shoulder B'. Exactly this scenario takes place upon the B $1s^{-1}2a_2''(\pi^*)$ excitation in BF_3[25–27] allowing for the observation of the B $1s\rightarrow 3a_1'$ transition.[24,28] In the present paper we focus mainly on the radiative decay of the N $1s^{-1}2a_2''(\pi^*)$ excitation.

The dots on the N 1*s* XA curve mark photon energies used for the excitation of RXE and nonresonant XE spectra shown in the lower panel of Fig. 2. The emission spectra are normalized to the acquisition time and the incoming photon flux. Processes of two types determine the shape of RXE spectra, which are commonly referred to as spectator and participator decay. The term ''spectator'' implies that the electron promoted from a core level to a near-edge unoccupied state remains in this state during the x-ray emission giving rise to RIXS structures in the spectra. In contrast, the ''participator'' electron returns from the near-edge state annihilating the core hole and causing resonant elastic x-ray scattering (REXS) (also called reemission or recombination) and, eventually, attendant inelastic processes. It is helpful for the following discussion to consider energy regions corresponding to the spectator and participator decay separately, since they almost do not overlap. Below the valence-band maximum position ($\sim$402 eV) all RXE structures are mainly due to the spectator x-ray emission, while above this value structures related to the participator process can also be observed. It is evident that the spectral shape dramatically changes in both energy regions upon scanning the photon energy across the N 1*s* edge.

Let us first compare the spectator part in the on-π^*-resonance spectrum (at 405.2 eV) with the corresponding region in the off-resonance spectrum (at 425.0 eV). Three main structures appear in the on-resonance spectrum: at 398.9 eV, at 393.6 eV and at 381.0 eV, which correspond to features *b* (MO $3e'$), *c* (MO's $2e'$ and $1a_2''$), and *e* (MO $1e'$) in the VB spectrum of Fig. 1, respectively. The validity of this assignment can be justified by the dipole selection rules for the transition from the excited $2A_2''$ state to the possible ''spectator'' final states of NO_3^- in the given experimental geometry assuming first for simplicity that the point group is still D_{3h}. It is enough to consider only electronic rules in order to account for the main three spectral features; however, vibronic coupling seems to be necessary to explain minor details. Three principally distinct orientations of the plane of the NO_3 group are possible: perpendicular to the photon-out direction (O1), perpendicular to the photon-in direction (O2), and in the plane determined by these two directions (O3). According to the electronic selection rules, in O1 the π^* excitation is allowed and one can see in RIXS the electron transitions only from MO's with the e' symmetry. In O2 and O3 the π^* excitation is forbidden, but if it would be allowed one could see in RIXS only the transitions from MO's with the a_2'' symmetry. In an intermediate orientation of the NO_3 group the π^* excitation is allowed, and the transitions from MO's with both e' and a_2'' symmetries should be observable in the emission spectra. We must be able to see both e' and a_2'' symmetries, because NO_3 groups were oriented randomly in our experiment. Since VB structures *b*, *c*, and *e* reflect electron transitions from the states with these two symmetries, they must dominate in RIXS via the $2A_2''$ intermediate state, provided that our quasimolecular description is valid. The fact that exactly this scenario takes place directly confirms that all major RIXS structures resulting from the radiative decay of this excitation in solid $LiNO_3$ can be qualitatively explained in the framework of a quasimolecular approach, i.e., in terms of MOs of the NO_3^- anion.

It should be noted that the positions of the main RIXS features are shifted to lower energies as compared to the nonresonant XES: band *b* is shifted by about 1 eV and band *c*− by 1.5 eV (band *e* is too broad to be properly evaluated). This negative spectator shift is an opposite of the positive one, which is commonly observed in the spectator Auger process. The negative shift has been observed previously, for example, in the B 1*s* RXES in B_2O_3 and hexagonal BN,[29] as well as in the RXES of gaseous N_2 (Ref. 30) and CO.[31] This phenomenon is probably rather general, at least for the systems with only *s* and *p* electrons. It reflects the fact that the ionization energy for the spectator electron is usually larger in the core-excited state than in the valence-excited (i.e., final) state.[31,32]

Another interesting feature in the on-π^*-resonance spectrum is a weak but evident shoulder on the low-energy side

of the most intense peak associated with the $2e'+1a_2''$ MO's. The energy position of this shoulder (392.3 eV) is close to that of the transition from the $2a_1'$ MO (corresponding to peak *d* in the VB XPS spectrum of Fig. 1), which has to be dipole forbidden in the D_{3h} symmetry. Therefore, the appearance of this shoulder may be indicative of the symmetry breaking in the $2A_2''$ state of the core-excited NO_3^- anion.

Upon tuning the excitation energy above the π^* resonance the RIXS spectrum experiences further evolution. While it looks similar to the normal XES curve at $h\nu_{in}=407.5$ eV, the changes in the spectral shape of RIXS excited at $h\nu_{in}=413.2$ eV (structure B in the N 1*s* XA spectrum) are considerable. For example, the structure at $h\nu_{out}=392.7$ eV and its low-energy tail become stronger, and a new peak appears at $h\nu_{out}=402.1$ eV. The identification of these features is more uncertain as compared to the case of deexcitation from the A_2'' state. They may be associated with a manifestation of the $2a_1'$ and $1e''$, $1a_2'$ MO's in the spectrum, indicating that the dipole selection rules are different from those for the case of $A_2''(\pi^*)$ excitation. On the other hand, solid-state effects can play a significant role too. Indeed, since the unoccupied states of the $LiNO_3$ crystal related to structures B and C are rather delocalized, the dispersion of the corresponding bands in the Brillouin zone may be sufficient for the momentum dependence to be seen. It is also quite probable that the shake-up satellites due to the excitation process (initial-state satellites) contribute considerably to the RIXS spectral shape as soon as the photon-in energies exceed the absorption threshold.

Let us now consider the part of the RXE spectra resulting from the deexcitation of the N $1s^{-1}2a_2''$ ($2A_2''$) state, which corresponds to the participator process. It is evident from Fig. 3 that the REXS (reemission) peak is accompanied by an intense structured low-energy tail at excitation energies close to the maximum of the π^* resonance. In order to facilitate the analysis of this loss structure we have fitted the reemission peak by a Gaussian with the full width at half maximum (FWHM) of 0.59 eV and subtracted it from the spectra. The result is shown in Fig. 4. The straight lines are provided as guidance for the eye, marking approximately energy positions of the beginning and the end of the loss structure.

We associate the losses observed in the resonant x-ray emission spectra shown in Figs. 3 and 4 to the manifestation of nuclear motion inside the core-excited NO_3^- species. There are two most possible scenarios of nuclear motion depending on whether the ground-state D_{3h} symmetry changes to C_{3v} upon the N $1s^{-1}2a_2''$ excitation or not. In both cases the N-O distances should increase upon promoting the core electron to the antibonding $2a_2''$ MO, so that one can expect a shift of the minimum of the potential energy surface for the corresponding vibronic states from the ground-state minimum.

If the point group symmetry remains unchanged, only the totally symmetric $\nu_1(a_1')$ stretching vibrations can be induced in NO_3, and it is the ν_1 vibrational progression, which determines the shape of the π^* absorption resonance (Fig. 2). The vibrational period of the ν_1 mode in the ground state

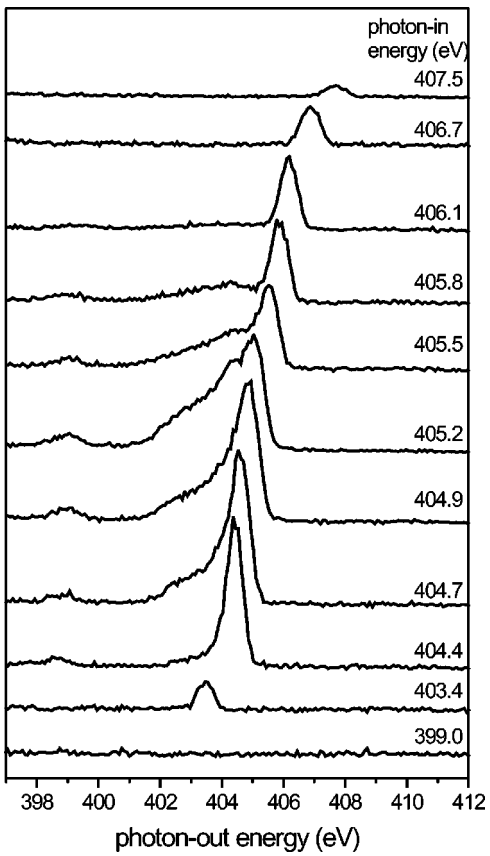

FIG. 3. Emission spectra reflecting elastic recombination and attendant inelastic processes.

of the free nitrate ion [32 fs (Ref. 33)] is comparable with the lifetime of the N $1s^{-1}\pi^*(\nu=0)$ excitation in simple N-containing molecules (N_2,N_2O), which is never shorter than 36 fs.[34] By analogy, it is quite probable that the period of the ν_1 mode in the core-excited NO_3^- anion is close to the lifetime of the N $1s^{-1}\pi^*(\nu=0)$ excitation in it. Thus, the loss structure observed in Figs. 3 and 4 may result from the x-ray emission during the symmetrical motion of the oxygen atoms away from the nitrogen atom in the plane of the anion.

Although this scenario cannot be excluded, we suggest another explanation based on the $D_{3h}\rightarrow C_{3v}$ symmetry breaking and vibronic coupling of the $1s^{-1}2a_2''$ and $1s^{-1}3a_1'$ states via the antisymmetric $a_2''(\nu_2)$ vibration (out-of-plane bending), because this mechanism has been revealed in the gas-phase BF_3 molecule,[25–27] which is isoelectronic and isostructural to NO_3^-. The $D_{3h}\rightarrow C_{3v}$ symmetry breaking was also observed in the quasimolecular [B*N_3] fragment of solid hexagonal BN upon the B $1s^{-1}a_2''$ core excitation.[35] Similar to the ν_1 mode, the a_2'' vibrational period in the ground state of the NO_3^- anion [40 fs (Ref. 33)] should be comparable with the lifetime of the N $1s^{-1}\pi^*(\nu=0)$ excitation, hence providing a necessary condition for the observation of x-ray emission caused by the very fact of the out-of-plane movement of the nitrogen atom. This issue is illustrated schematically in Fig. 5. We consider only the absorption transitions from the vibronic ground state ($\nu=0$) into the excited $2A_2''$ state, which potential energy curve

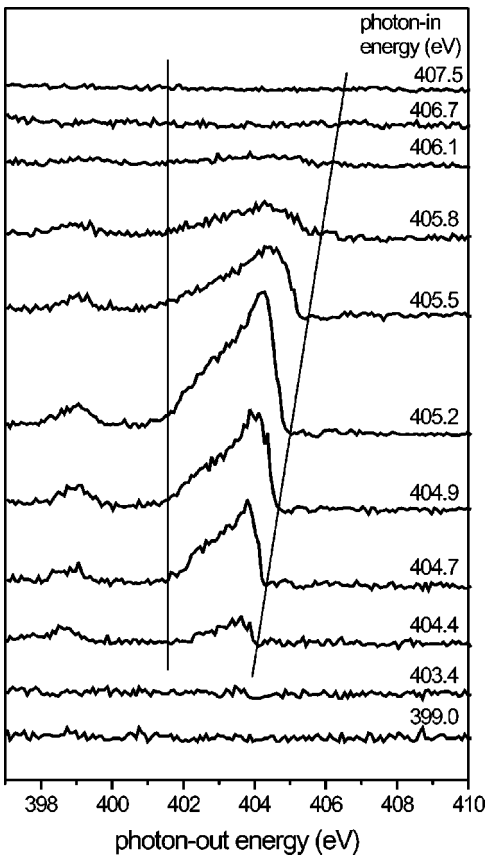

FIG. 4. Spectra of Fig. 3 after subtraction of the reemission peak.

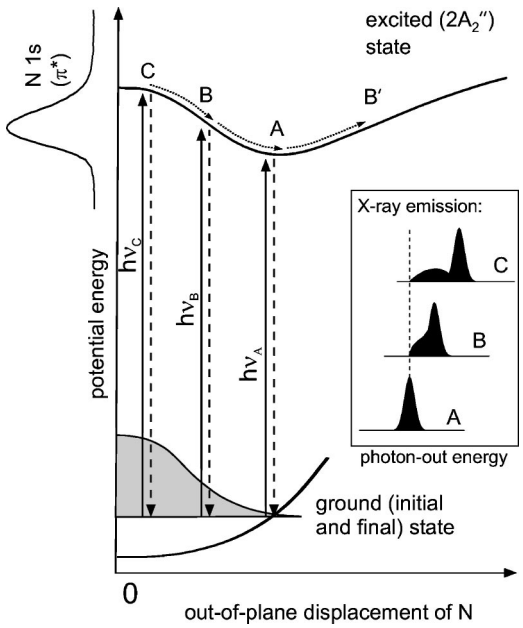

FIG. 5. Schematic of excitation of the NO_3^- anion to the $2A_2''$ intermediate state followed by the transition back to the ground state. Area under the vibrational wave function in the ground state is shadowed. Inset illustrates the origin of the dynamical emission satellite.

is supposed to have a minimum in a nonzero point on the axis of the out-of-plane displacement of the nitrogen atom, as it was found for BF_3.[26,27] In the reemission process the final electronic state is the same as the ground state, however the transitions to the nonzero vibrational levels of the ground state are not forbidden. These transitions may probably contribute to the loss feature in Figs. 3 and 4, but they cannot explain its behavior upon scanning the photon-in energy across the resonance. Indeed, the loss feature does not follow the reemission peak as it would do if it reflected merely the transitions to the nonzero vibrational levels of the ground state. Instead, the position of its low-energy edge remains unchanged, while the overall extent of the loss feature gradually increases. Besides, the intensity of the losses becomes unusually high around the resonance maximum: their integral strength exceeds the intensity of the reemission peak itself in the on-resonance spectrum at $h\nu_{in}=405.2$ eV (Fig. 3). (However, it should be noted that the reemission peak strength is probably reduced due to the self-absorption in the region of π^* resonance.) We suggest that the reason for this behavior is an essentially dynamical process based on the fact that the emission can occur simultaneously with the NO_3^- bending distortion along the potential curve of the excited state. As long as the excitation energy is just sufficient for the absorption to occur (to point *A* in Fig. 5), only the recombination peak itself can be seen in the RXES (the curve excited with $h\nu_{in}=403.4$ eV in Fig. 3). Both absorption and recombination are weak at this point, because it is only the tail of the ground state vibronic wave function, which gives rise to the transitions. As the photon-in energy increases, the out-of-plane bending inside NO_3 becomes possible, and the x-ray emission can occur now at any point on the potential energy curve between the classical inner and outer turning points resulting in a low-energy tail of the reemission peak. For example, the excitation to point *B* on the potential energy curve can decay at any time as the system evolves along the way *B*-*A*-*B′* and back (Fig. 5). Further increase in the photon-in energy results in the elongation of the low-energy tail as shown schematically in the inset to Fig. 5 and can be seen directly in the data in Fig. 4. It should be noted that in the resonant Auger decay the emission from both turning points (like *B* and *B′*) can be probably seen in the core-excited NO_3^- anion,[16] while in RXES only the part between the inner turning point and the minimum of the potential energy curve is observable (as a consequence of different final states).

Because of the essentially dynamical nature of the observed effect, it can be called *dynamical x-ray emission* by analogy with the process of dynamical Auger emission observed first for BF_3 (Ref. 36) and then for other simple molecules.[37,38] A similar effect has been observed by Ma *et al.* in the radiative recombination of the C 1*s* core exciton of diamond[39] being attributed by Tanaka and Kayanuma to the x-ray emission during the off-center displacement of the core-excited carbon atom in course of the $T_d \rightarrow C_{3v}$ distortion.[40] Although the dynamical x-ray emission is relevant not only for ionic-molecular crystals, these compounds seem to be particularly suitable for its investigation due to

the quasimolecular character of their electronic structure and nature of core excitations.

IV. CONCLUSIONS

In this work we investigated resonant x-ray emission resulting from the core excitations at the nitrogen $1s$ edge in the ionic-molecular solid $LiNO_3$. It has been shown that the origin of main RIXS structures can be explained in the framework of a quasimolecular approach, i.e., in terms of molecular orbitals of the NO_3^- anion. The majority of these structures can be explained assuming undistorted D_{3h} geometry of the core-excited NO_3^- species (evidently, the corresponding transitions must be allowed in the C_{3v} geometry too). A weak signal appears in the on-π^*-resonance spectrum at the position of electron transitions from the $2a_1'$ MO indicating possibly that this transition becomes dipole-allowed as a consequence of the C_{3v} bending.

In the reemission spectrum an intense structured tail extending over about 3 eV has been observed at the low-energy side of the reemission peak upon tuning the photon-in energy to the maximum of the N $1s \rightarrow \pi^*$ absorption resonance. This sideband is assigned mainly to the effect of dynamical x-ray emission, i.e., the emission from the different points of the potential energy curve of the core-excited state; however a contribution from the transitions to the nonzero vibrational levels of the electronic ground state cannot be excluded. The most probable scenario is the x-ray emission accompanying the out-of-plane movement of the nitrogen atom in course of the $D_{3h} \rightarrow C_{3v}$ distortion of the core-excited NO_3^- species.

ACKNOWLEDGMENTS

The authors are grateful to Dr. T. Kaambre for the valuable assistance with experiments. This work was supported by the Russian Foundation for Basic Research (Grant No. 01-03-32285), Deutsche Forschungsgemeinschaft (Grant No. FOR 404), and the Swedish Research Council and the Swedish Foundation for Strategic Research. A. B. Preobrajenski gratefully acknowledges the support by the Swedish Foundation for International Cooperation in Research and Higher Education (STINT).

*Electronic address: alexeip@maxlab.lu.se

[1] P.D. Johnson and Y. Ma, Phys. Rev. B **49**, 5024 (1994).
[2] E.L. Shirley, J. Electron Spectrosc. Relat. Phenom. **110-111**, 305 (2000).
[3] Y. Ma, N. Wassdahl, P. Skytt, J. Guo, J. Nordgren, P.D. Johnson, J.-E. Rubensson, T. Boske, W. Eberhardt, and S.D. Kevan, Phys. Rev. Lett. **69**, 2598 (1992).
[4] J.A. Carlisle, E.L. Shirley, L.J. Terminello, E.A. Hudson, J.J. Jia, T.A. Callcott, D.L. Ederer, R.C.C. Perera, and F.J. Himpsel, Phys. Rev. Lett. **74**, 1234 (1995).
[5] J.A. Carlisle, S.R. Blankenship, L.J. Terminello, J.J. Jia, T.A. Callcott, D.L. Ederer, R.C.C. Perera, and F.J. Himpsel, J. Electron Spectrosc. Relat. Phenom. **110-111**, 323 (2000).
[6] J.J. Jia, T.A. Callcott, E.L. Shirley, J.A. Carlisle, L.J. Terminello, A. Asfaw, D.L. Ederer, F.J. Himpsel, and R.C.C. Perera, Phys. Rev. Lett. **76**, 4054 (1996).
[7] P.A. Brühwiler, P. Kuiper, O. Eriksson, R. Ahuja, and S. Svensson, Phys. Rev. Lett. **76**, 1761 (1996).
[8] M. van Veenendaal and P. Carra, Phys. Rev. Lett. **78**, 2839 (1997).
[9] A. Kotani, J. Electron Spectrosc. Relat. Phenom. **110-111**, 197 (2000).
[10] A. Kotani and S. Shin, Rev. Mod. Phys. **73**, 203 (2001).
[11] S.M. Butorin, J.-H. Guo, M. Magnuson, P. Kuiper, and J. Nordgren, Phys. Rev. B **54**, 4405 (1996).
[12] S.M. Butorin, D.C. Mancini, J.-H. Guo, N. Wassdahl, J. Nordgren, M. Nakazawa, S. Tanaka, T. Uozumi, A. Kotani, Y. Ma, K.E. Myano, B.A. Karlin, and D.K. Shuh, Phys. Rev. Lett. **77**, 574 (1996).
[13] A. Moewes, D.L. Ederer, M.M. Grush, and T.A. Callcott, Phys. Rev. B **59**, 5452 (1999).
[14] A.S. Vinogradov, A.B. Preobrajenski, S.L. Molodtsov, S.A. Krasnikov, R. Szargan, A. Knop-Gericke, and M. Hävecker, Chem. Phys. **249**, 249 (1999).
[15] A.B. Preobrajenski, A.S. Vinogradov, S.L. Molodtsov, S.A. Krasnikov, T. Chassè, R. Szargan, and C. Laubschat, Phys. Rev. B **65**, 205116 (2002).
[16] A.B. Preobrajenski, A.S. Vinogradov, S.L. Molodtsov, S.A. Krasnikov, R. Szargan, and C. Laubschat, Chem. Phys. Lett. **368**, 125 (2003).
[17] N. Kosuch, E. Tegeler, G. Wiech, and A. Faessler, J. Electron Spectrosc. Relat. Phenom. **13**, 263 (1978).
[18] M.P. Keane, A. Naves de Brito, N. Correia, S. Svensson, L. Karlsson, B. Wannberg, U. Gelius, S. Lunell, W.R. Salaneck, M. Logdlund, D.B. Swanson, and A.G. MacDiarmid, Phys. Rev. B **45**, 6390 (1992).
[19] M. Ehara, Y. Ohtsuka, and H. Nakatsuji, Chem. Phys. **226**, 113 (1998).
[20] P. Tomasello, M. Ehara, and H. Nakatsuji, Chem. Phys. **118**, 5811 (2003).
[21] J.F. Wyatt, I.H. Hillier, V.R. Saunders, J.A. Connor, and M. Barber, J. Chem. Phys. **54**, 5311 (1971).
[22] S.P. Dolin and M.E. Dyatkina, J. Struct. Chem. **13**, 906 (1972).
[23] L.E. Harris, J. Chem. Phys. **58**, 5615 (1973).
[24] E. Ishiguro, S. Iwata, Y. Suzuki, A. Mikuni, and T. Sasaki, J. Phys. B **15**, 1841 (1982).
[25] M. Simon, P. Morin, P. Lablanquie, M. Lavollee, K. Ueda, and N. Kosugi, Chem. Phys. Lett. **238**, 42 (1995).
[26] M. Simon, C. Miron, N. Leclercq, P. Morin, K. Ueda, Y. Sato, S. Tanaka, and Y. Kayanuma, Phys. Rev. Lett. **79**, 3857 (1997).
[27] S. Tanaka, Y. Kayanuma, and K. Ueda, Phys. Rev. A **57**, 3437 (1998).
[28] K. Ueda, in *Atomic and Molecular Photoionization*, edited by A. Yagishita and T. Sasaki (Universal Academy Press, Tokyo, 1996), p. 139.
[29] W.L. O'Brien, J. Jia, Q.-Y. Dong, T.A. Callcott, K.E. Miyano, D.L. Ederer, D.R. Mueller, and C.-C. Kao, Phys. Rev. Lett. **70**, 238 (1993).
[30] P. Glans, P. Skytt, K. Gunnelin, J.-H. Guo, and J. Nordgren, J. Electron Spectrosc. Relat. Phenom. **82**, 193 (1996).

[31] P. Skytt, P. Glans, K. Gunnelin, J.-H. Guo, J. Nordgren, Y. Luo, and H. Ågren, Phys. Rev. A **55**, 134 (1997).
[32] H. Ågren, Y. Luo, F. Gel'mukhanov, and H.J.A. Jensen, J. Electron Spectrosc. Relat. Phenom. **82**, 125 (1996).
[33] G.E. Ahlijah and E.F. Mooney, Spectrochim. Acta, Part A **25**, 619 (1969).
[34] K.C. Prince, M. Vondracek, J. Karvonen, M. Coreno, R. Camilloni, L. Avaldi, and M. de Simone, J. Electron Spectrosc. Relat. Phenom. **101-103**, 141 (1999).
[35] A.A. Pavlychev, R. Franke, S. Bender, and J. Hormes, J. Phys.: Condens. Matter **10**, 2181 (1998).
[36] K. Ueda, H. Chiba, Y. Sato, T. Hayaishi, E. Shigemasa, and A. Yagishita, J. Chem. Phys. **101**, 3520 (1994).
[37] C. Miron, R. Guillemin, N. Leclercq, P. Morin, and M. Simon, J. Electron Spectrosc. Relat. Phenom. **93**, 95 (1998).
[38] K. Ueda, S. Tanaka, Y. Shimizu, Y. Muramatsu, H. Chiba, T. Hayaishi, M. Kitajima, and H. Tanaka, Phys. Rev. Lett. **85**, 3129 (2000).
[39] Y. Ma, P. Skytt, N. Wassdahl, P. Glans, D.C. Mancini, J. Guo, and J. Nordgren, Phys. Rev. Lett. **71**, 3725 (1993).
[40] S. Tanaka and Y. Kayanuma, Solid State Commun. **100**, 77 (1996).